

EGYPTIAN JOURNAL OF BOTANY (EJBO)

Therapeutic potential of *Lactobacillus plantarum* HBUAS68394 in mitigating DSSinduced colitis

Fatma E.A. Yousef¹, Mohammed A. Hussein², Reda M. Taha¹, Mai Ali Mwaheb¹

¹Botany Department, Faculty of Science, Fayoum University, Fayoum ARTICLE HISTORY 63514, Egypt

²Biotechnology Department, Faculty of Applied Heath Science Technology, October 6 University, Giza 28125, Egypt

Inflammatory bowel diseases (IBD), including colitis, are characterized by persistent gastrointestinal inflammation, contributing to substantial health complications. Existing therapies frequently show restricted effectiveness and undesirable side effects, highlighting the need for alternative treatments. This study investigated the potential of Lactobacillus plantarum HBUAS68394 and celebrex in alleviating DSS-induced colitis in a murine model.

The mice were treated with Dextran sulfate sodium (DSS) to induce colitis, followed by administration of L. plantarum and celebrex. Colon EDITED BY: Mohamed Khaled Ibrahim tissue integrity was evaluated via histology, PCR, and biochemical tests, measuring inflammatory cytokines (TNF-α, IL-1β, IL-12, NF-κB, HMGB1, cAMP, MPO), oxidative stress indicators (MDA, GSH, SOD), lipid profiles (cholesterol, triglycerides), and gut barrier markers (TFF3).

Results demonstrated that L. plantarum and celebrex effectively reduced colitis severity in DSS-treated mice. Microscopic examination showed improved colon architecture, including intact crypts and diminished inflammatory infiltration. PCR results showed decreased levels of TNF-α, IL-1β, IL-12, cAMP, MPO, and MDA, as well as gene expression of NF-κB and HMGB1 proteins. Additionally, there was increased expression of the mucosal protective factor TFF3, as well as levels of GSH and SOD. Both treatments also improved lipid profiles by reducing plasma triglycerides and cholesterol levels and enhanced gut barrier function.

The findings underscore the potential of L. plantarum HBUAS68394 and celebrex as therapeutic agents for managing colitis and enhancing colon health. This study provides a foundation for future clinical applications and personalized treatment strategies for inflammatory bowel diseases, aiming to improve patient outcomes and quality of life.

Keywords: DSS, Inflammatory cytokines, Lactobacillus plantarum, Oxidative stress biomarkers, TFF3, Ulcerative colitis

INTRODUCTION

Inflammatory bowel diseases (IBD), including colitis. are characterized by persistent gastrointestinal inflammation, contributing to substantial health complications (Creighton et al., 2010). Existing therapies frequently show restricted effectiveness and undesirable side effects, highlighting the need for alternative

Submitted: March 3, 2025 Accepted: September 2, 2025

CORRESPONDANCE TO:

Mohammed A. Hussein Biotechnology Department, Faculty of Applied Heath Science Technology, October 6 University, Giza 28125, Egypt Email: prof.husseinma@o6u.edu.eg

DOI: 10.21608/ejbo.2025.363646.3211

treatments (Ghosh & Mitchell, 2007). Dextran sulfate sodium (DSS)-induced colitis is a widely used murine model that mimics human ulcerative colitis (UC) by disrupting the epithelial barrier and triggering immune responses, making it ideal for testing therapeutic interventions like probiotics (Danese, 2011).

Recent investigations in murine models have Egypt. J. Bot., Vol. 65, No. 4, pp. 261-275 (2025)

identified leucine-rich alpha-2-glycoprotein (LRG), interleukin-1 β (IL-1 β), and interleukin-12 (IL-12) as critical biomarkers correlating with disease severity and inflammatory activity (Takahiro et al., 2023). These molecular indicators not only reflect disease progression but also represent potential therapeutic targets for intervention strategies (Satohiro & Hirosato, 2022).

The oxidative stress paradigm in UC involves several key mediators. The antioxidant system components glutathione (GSH) and superoxide dismutase (SOD) serve protective functions against oxidative damage, while malondialdehyde (MDA) accumulates as a byproduct of lipid peroxidation, reflecting cellular injury (Muro et al., 2024). The inflammatory cascade in UC involves multiple signaling pathways, including cAMP-mediated cellular signaling that modulates immune responses, tumor necrosis factor-alpha (TNF- α) driven tissue inflammation (Lu et al., 2020), and myeloperoxidase (MPO)-generated reactive oxygen species (Yang et al., 2022)

At the molecular level, nuclear factor kappa-B (NF- κ B) activation initiates pro-inflammatory cytokine production, perpetuating chronic inflammation (Nakov et al., 2019). Concurrently, altered expression of trefoil factor 3 (TFF3) impairs mucosal repair mechanisms, while high mobility group box 1 (HMGB1) protein exacerbates inflammatory responses when released into extracellular spaces (VanPatten & Al-Abed, 2018; Yang et al., 2022).

Therapeutic interventions targeting these pathways show promise. Probiotic formulations demonstrate multimodal benefits by: Suppressing pro-inflammatory mediators (TNF- α , MPO), augmenting antioxidant capacity (GSH, SOD), and stimulating mucosal repair factors (TFF3).

Among probiotic strains, *Lactobacillus plantarum* has emerged as a particularly effective candidate due to its documented anti-inflammatory properties, efficacy in managing functional bowel disorders, immune-modulating capabilities, and protective effects against enteric pathogens (Ilavenil et al., 2015; Mendoza et al., 2019; Nordström et al., 2021).

Lactobacillus plantarum HBUAS68394 was selected based on its documented probiotic properties, including bile salt tolerance, adhesion capability, and anti-inflammatory effects in prior studies (Fidanza et al., 2021). This strain's ability

to modulate gut microbiota and immune responses made it a promising candidate for UC management.

This study specifically examines the therapeutic potential of *L. plantarum* strain HBUAS68394 in a dextran sulphate sodium (DSS)-induced murine colitis model. Through comprehensive evaluation of its effects on inflammatory pathways, oxidative stress parameters, and mucosal healing processes, we aim to establish its viability as an adjunctive treatment for UC.

MATERIALS AND METHODS Materials

The *L. plantarum HBUAS68394* strain was procured from the Microbial Inoculants Center at Ain Shams University, Cairo, Egypt. For bacterial cultivation, we employed de Man, Rogosa, and Sharpe (MRS) medium (Sigma-Aldrich, USA), with all chemical reagents meeting analytical-grade specifications. The probiotic strain was cultured in 100 mL of MRS broth under aerobic conditions, maintained at 37°C for 18-24h with constant orbital shaking at 150 rpm to ensure optimal growth conditions.

Culture and extraction of L. plantarum biomass

Following incubation, bacterial cells were harvested through centrifugation at $2800 \times g$ for 10 min at 4°C to pellet the biomass. The resulting cell pellet was carefully separated from the culture supernatant and divided into two aliquots: one portion reserved for comprehensive strain characterization and the remainder allocated for subsequent biological activity assessments.

Characterization of L. plantarum Identification using 16S rRNA gene sequence

For molecular identification, genomic DNA extraction was performed using the QIAamp DNA Mini Kit (Qiagen, USA) following the manufacturer's protocol. The 16S rRNA gene was amplified using universal bacterial primers 27F and 1492R, generating an approximately 1500 bp amplicon. PCR products were purified and subjected to bidirectional sequencing using an ABI PRISM 3730XL Genetic Analyzer with BigDye Terminator chemistry (Life Technologies, UK). Sequence data were analyzed through BLASTn comparison against the NCBI nucleotide database, and phylogenetic relationships were reconstructed using appropriate bioinformatics tools.

To confirm amplification success, PCR products were electrophoresed on 1% agarose gels and visualized under UV illumination. Additional

verification was performed using capillary electrophoresis on an ABI 3730xl Genetic Analyzer (Microgen, UK) to ensure fragment size accuracy. The complete 16S rDNA sequence was deposited in GenBank under accession number OR835817.1, add 99.35% similarity to reference *L. plantarum* strains (Table 1).

Bile salt tolerance assessment

We evaluated the bile resistance capacity of *L. plantarum* following established protocols (Leite et al., 2015) with modifications. After growing the culture overnight to achieve 10⁸ CFU/mL density, cells were pelleted by centrifugation (10,000 × g, 5min, 4°C) and resuspended in phosphate-buffered saline (PBS, pH 6.5) to OD600= 0.5. The bacterial suspensions were exposed to varying oxgall concentrations (0.05-0.30% w/v) and incubated at 37°C for 1-3h. Viability was assessed by plating serial dilutions on both standard MRS agar and bile-supplemented media. Bacterial survival rates were calculated using the logarithmic ratio of final to initial colony counts:

Survival (%)= (log CFU/mLfinal \div log CFU/mLinitial) \times 100

Cell surface hydrophobicity determination

The adhesive properties of *L. plantarum* were examined according to published methodology (Abbasiliasi et al., 2017). Bacterial suspensions (10⁸ CFU/mL in PBS, pH 7.2) were combined with organic solvents (n-hexadecane, chloroform, ethyl acetate) in 1:5 ratios. Following vigorous vortexing (1min) and phase separation (5-10min), aqueous phase absorbance was measured at 600nm (Shimadzu UV-1800) before and after incubation (37°C, 10min). Hydrophobicity was quantified as:

Adhesion (%) = $[1 - (A10min/A0min)] \times 100$

Haemolytic activity screening

Safety evaluation included haemolysis testing on sheep blood agar plates (5% v/v erythrocytes). Aliquots (50 μ L) of bacterial suspension (108 CFU/mL) were spot-inoculated and incubated (37°C, 48h) before examining zones of haemolysis.

Probiotic administration

- Dosing Rationale: The dose of L. plantarum (10^8 CFU/mL) was chosen based on previous studies demonstrating efficacy in murine colitis models without adverse effects (Yang et al., 2022).
- Mice received *L. plantarum* orally via gavage once daily for 15 days, suspended in distilled water to ensure consistent delivery. Control groups received equivalent volumes of water or DSS (5% in drinking water).

Celebrex administration:

• The dose of celecoxib (10mg/kg) was selected to match standard anti-inflammatory protocols (Li et al., 2024), though its partial efficacy may reflect COX-2 inhibition's limited impact on DSS-induced oxidative stress pathways.

Animal experimental design

The study utilized thirty male C57BL/6 mice $(35 \pm 2.5g)$ obtained from the National Cancer Institute (Cairo University). Following 10-day acclimation under controlled conditions $(22 \pm 2^{\circ}\text{C}, 60\% \text{ humidity}, 12:12 \text{ light-dark cycle})$ with ad libitum access to standard chow (Dyets Inc., USA), animals were randomly allocated into five experimental groups (n=6/group) (Table 2):

Blood sample processing

On day 16, we collected blood samples (0.4mL/ mouse) via retro-orbital puncture from etheranesthetized animals into heparinized tubes. Plasma separation was achieved by centrifugation at 1,000 × g for 20min at 4°C. We quantified plasma lipid profiles (total cholesterol, triglycerides, HDL cholesterol) using enzymatic colorimetric assays (Asan Pharmaceutical/Youngdong, Korea). Inflammatory mediators (LRG, IL-1β, IL-12, cAMP, TNF-α) were measured with commercial ELISA kits from multiple suppliers: LRG: Biomedica (Cat# 220524), IL-1β: Abcam (Cat# ab100704), IL-12: Novus Biologicals (Cat# NBP1-92677), cAMP: FineTest (Cat# EU2574), and TNF-α: Abcam (Cat# ab208348)

Table 1. Primer sequence

Primer's code	Sequence	Product Size
27F	5'- AGAGTTTGATCCTGGCTAG -3'	15001
1492R	5'- GGTTACCTTGTTACGACTT -3'	1500 bp

NCBI Reference: The 16S rRNA gene sequence of *Lactobacillus plantarum* HBUAS68394 was deposited in GenBank under accession number OR835817.1 (accessed on 22-Nov-2023).

Table 2. Description of treatment groups

Groups	Treatment description	Treatment Description
I	Control group	Mice administrated a normal diet for 15 days.
II	L. Plantarum (10 ⁸ CFU/mL)	Mice were received <i>L. plantarum</i> (10 ⁸ CFU/mL), suspended in distilled water over 15 days (Yang et al., 2022).
III	DSS (5% in drinking water)	Colitis was induced in mice using DSS (5% in drinking water, orally for 15 days (Metwaly et al., 2022).
IV	DSS + L. Plantarum (10 ⁸ CFU/mL)	Colitis was induced in mice using DSS, after which they received L . plantarum (10 8 CFU/mL)
V	DSS + Celebrex (10mg/kg.b.w.)	Colitis was induced in mice using DSS, after which they received celebrex intervention (10 mg/kg.b.w.) suspended in distilled water for over 15 days (Li et al., 2024).

Tissue processing and preservation

Following euthanasia, we excised colons and performed PBS-perfusion to remove luminal contents. After blot-drying between filter papers, each colon was divided longitudinally:

Distal segment: Fixed in 10% neutral buffered formalin for histopathology

Proximal segment: Flash-frozen in liquid nitrogen and stored at -80°C for oxidative stress markers (MDA, GSH, SOD) and gene expression analysis (NF-κB, HMGB1, TFF3)

Molecular biology procedures RNA isolation and cDNA synthesis

Total RNA extraction from frozen colon tissues was performed using the RNA-spinTM purification system (Qiagen, Germany). RNA integrity was verified b A260/A280 ratio (1.8-2.0). For reverse transcription, 5μg total RNA was converted to cDNA using the High-Capacity cDNA Reverse Transcription Kit (Applied Biosystems, USA).

Quantitative real-time PCR

We performed qPCR reactions in triplicate using: SYBR Green Master Mix (iNtRON Biotechnology, Korea), Gene-specific primers (Table 3), β -actin as endogenous control (PrimerDesign, USA), and thermocycling conditions:

Initial denaturation: 95°C for 10 min, 40 cycles of 95°C for 15 sec, 60°C for 1min and melt curve analysis 60-95°C

Histopathological evaluation

Colonic tissue samples underwent standard

histological processing: fixation in 10% neutral buffered formalin, paraffin embedding, and sectioning at 5µm thickness. Hematoxylin and eosin staining (H&E) revealed distinct morphological differences between experimental groups. DSS-treated animals (Group III) showed marked pathology including Crypt architectural distortion (37.2% reduction in normal crypts), epithelial cell pyknosis (2.3-fold increase vs controls).

Statistical analysis

All quantitative data are presented as mean \pm SD (n=6/group). We performed one-way ANOVA with Tukey's post-hoc test using SPSS v20 (IBM), considering P<0.05 statistically significant.

RESULTS

16S rRNA identification of L. plantarum

To determine the identity of the *L. plantarum HBUAS68394 strain*, phylogenetic analysis was employed using BLAST (Figure 1). Figure 2 shows that the maximal sequence similarity of a 1500 bp fragment of the 16S rRNA gene used for genotypic identification by gene sequencing was 99.35% to the GenBank reference strain *L. plantarum* with accession number OR835817.1.

Bile salt tolerance test

The *L. plantarum HBUAS68394 strain* was subjected to different oxgall concentrations (0.10-0.30%) at incubation times of 1, 2, and 3h. As shown in Figure 3, the *L. plantarum HBUAS68394 strain*conferred the highest survival rates of more than 82%, 92%, and 96% at 0.30% bile concentrations after incubation for 1, 2, and 3h, respectively.

Table 3. Primer sequences used for qPCR analysis of NF- κ B, HMGB1, TFF3, and β -actin

Gene	Forward Primer (5'→3')	Reverse Primer (5'→3')	Reference/ Source
NF-κB	CATGAAGAGAAGACACTGACCATGGAAA	TGGATAGAGGCTAAGTGTAGACACG	Designed using Primer-BLAST
HMGB1	TGATTAATGAATGAGTTCGGGC	TGCTCAGGAAACTTGACTGTTT	Adapted from (NCBI feature table guidelines)
TFF3	TAATGCTGTTGGTGGTCCTG	CAGCCACGGTTGTTACACTG	Validated via PrimerBank
β-actin	TGACTGACTACCTCATGAAGATCC	TCTCCTTAATGTCACGCACGATT	Housekeeping gene; cited in (genomic research methods)

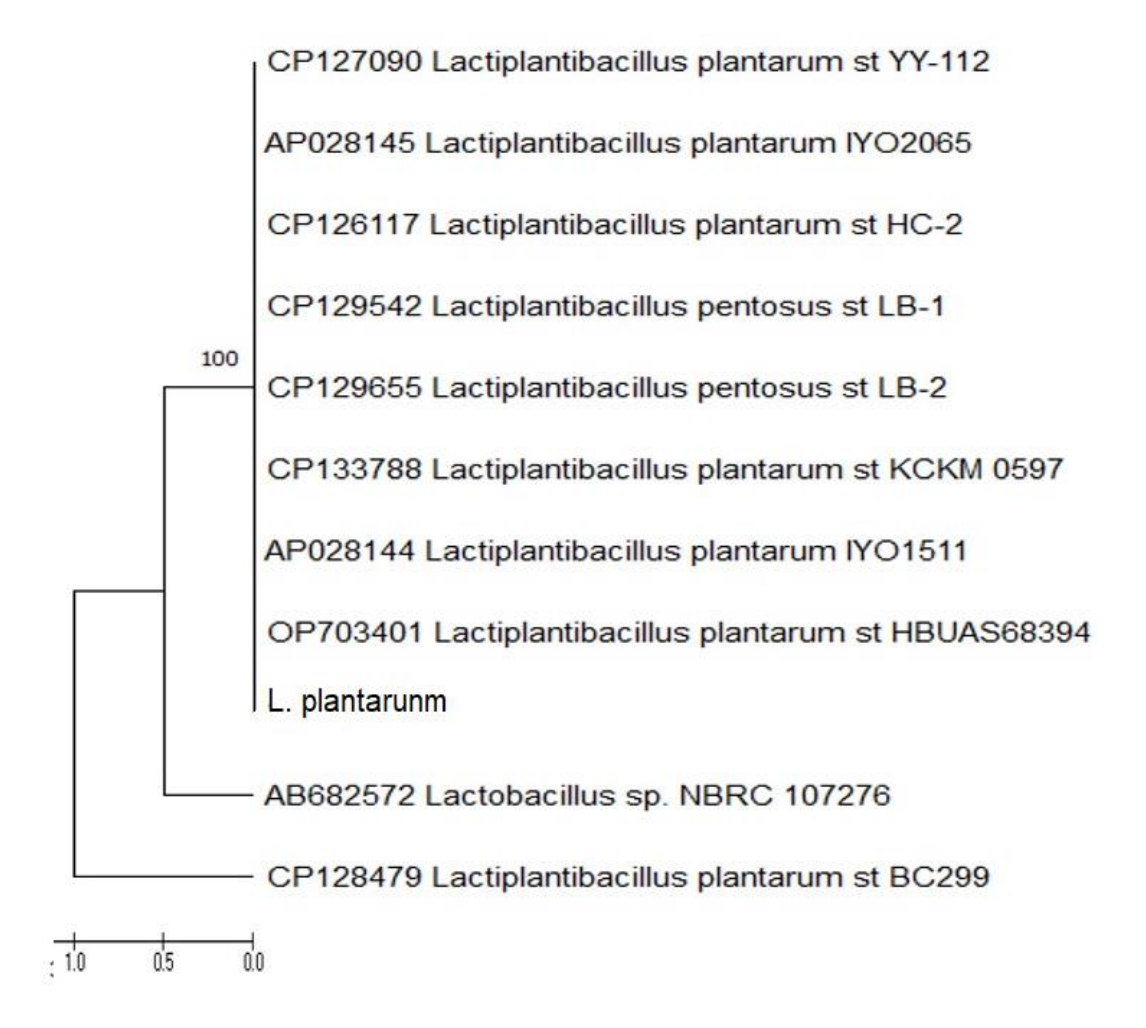


Figure 1. Phylogenetic tree based on 16S rRNA gene sequences showing the evolutionary position of *Lactobacillus plantarum* HBUAS68394 (OR835817.1) among related bacterial strains

Egypt. J. Bot., Vol. 65, No. 4 (2025)

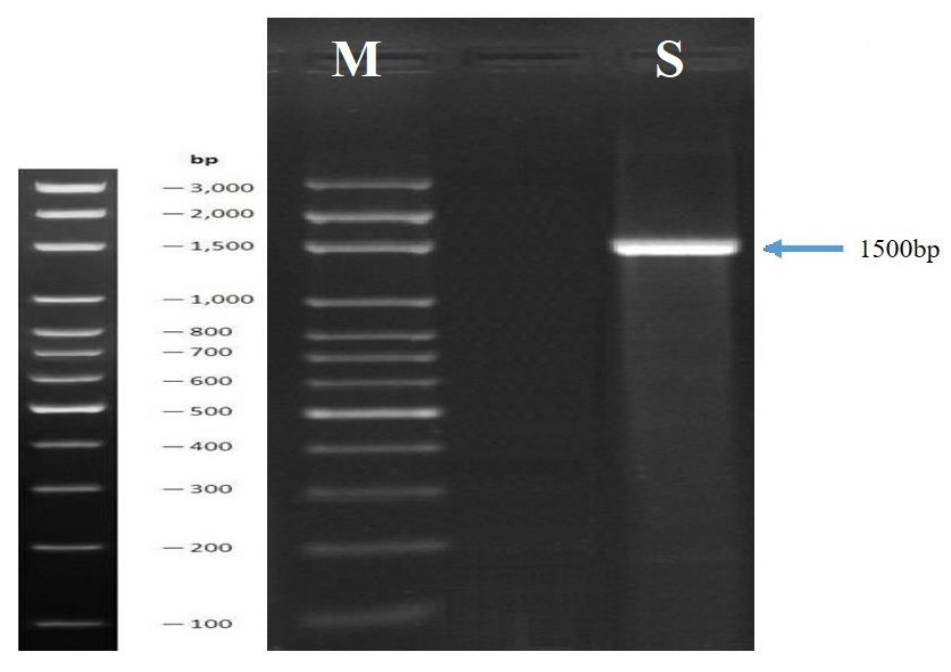


Figure 2. The bands corresponding to the amplified sequences in the PCR reaction (M: DNA ladder: 50 bp, S: band *L. plantarum*, about 1500 bp.)

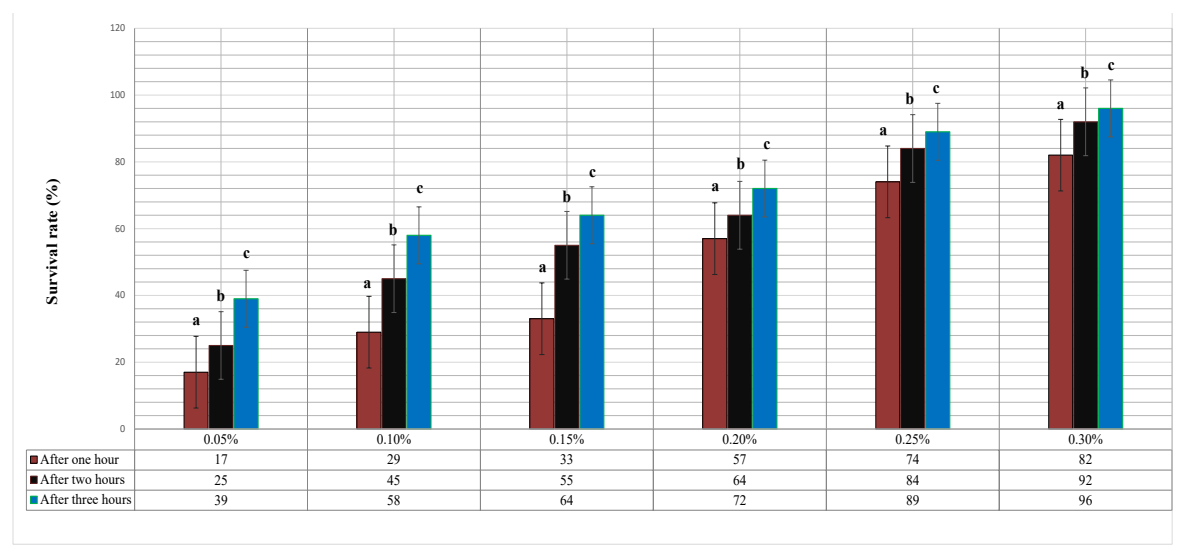


Figure 3. Survival rates of *L. plantarum* HBUAS68394 (in bile salt (0.05-0.30%) conditions for 1, 2, and 3h. [Values represent the mean \pm SD (n=3). Data followed by the same letter are not significantly different at $P \le 0.05$. The high significant levels of the parameters were in the order of a < b < c. Data with superscript alphabet "a" are significantly lower than data with superscript alphabet "b" while data with superscript "b" are lower than data with superscript alphabet c at *P<0.05]

Assay of L. plantarum affinity to solvents

The findings from Figure 4 show that *L. plantarum* exhibits varying affinities to different solvents, and this affinity changes over time. *L. plantarum* has the highest affinity for ethyl acetate, followed by n-hexadecane, and then chloroform. As incubation time increases (10, 20, 30, and 40min), the affinity of *L. plantarum* to the solvents also increases.

The affinity percentages of *L. plantarum* to ethyl acetate, chloroform, and n-hexadecane were 36%, 91%, and 92%, respectively, after 40min of incubation. This suggests that the interaction of *L. plantarum* with the solvents becomes stronger over time. Hydrophobicity and Lewis acid-base characteristics play a crucial role in *L. plantarum* adhesion to surfaces.

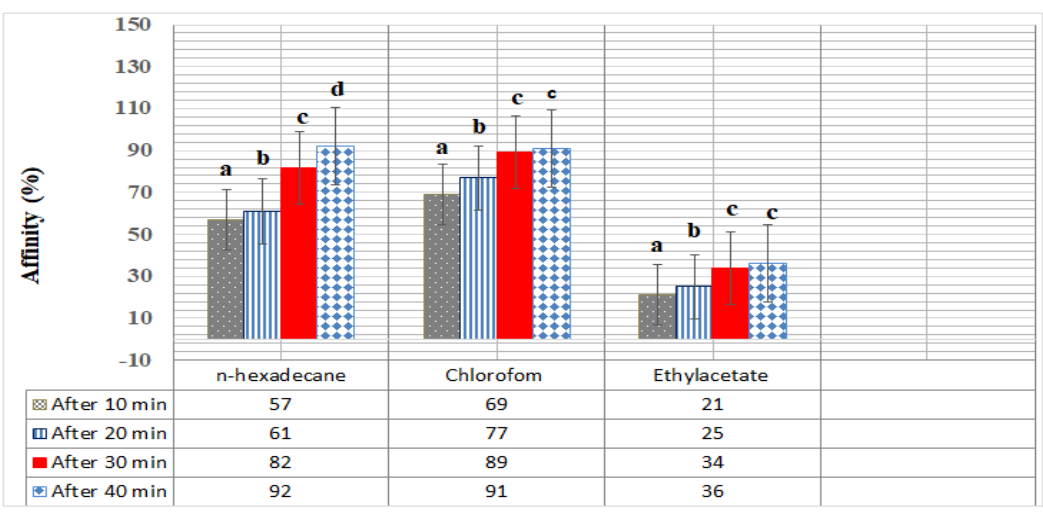


Figure 4. Adhesion assay of $\it L. plantarum \, HBUAS68394$ to solvents (n-hexadecane, chloroform and ethyl acetate). [Values represent the mean $\pm \, SD \, (n=3)$. Data followed by the same letter are not significantly different at $P \le 0.05$. The high significant levels of the parameters were in the order of a < b < c . Data with superscript alphabet "a" are significantly lower than data with superscript alphabet "b" while data with superscript "b" are lower than data with superscript alphabet c and at *P < 0.05]

Hemolytic activity of L. plantarum

In the current investigation, L. plantarum was tested for hemolysis on agar blood plates. The results indicated that L. plantarum did not exhibit any hemolysis on these plates. This absence of hemolysis suggests that L. plantarum does not cause damage to red blood cells. The fact that L. plantarum was γ -hemolytic (no hemolysis) aligns with its non-pathogenic nature.

Effect of L. plantarum on mice's body weight

The current findings in Table 4 showed the changes in body weight of mice when treated with *L. plantarum*. In the normal mice treated with *L. plantarum* (10⁸ CFU/mL), the body weight did not significantly change compared to normal mice. The DSS-treated mice experienced a significant decrease in body weight by 34.04% compared to the DSS-treated group. When compared to the DSS-treated group, oral administration of *L. plantarum* (10⁸ CFU/mL) resulted in a significant increase (P<0.05) in body weight by 42.0%. Additionally, administration of DSS-treated mice with celebrex (10mg/kg) significantly increased body weight by 38.41% compared to the DSS-treated group.

Effect of *L. plantarum* HBUAS68394 and Celebrex on plasma TC, TG, and HDL-C in treated mice

Table 5 showed plasma levels of TC, TG, and HDL-C in different groups of mice. When compared to the normal control group, oral administration of DSS (5%) resulted in a significant

decrease (P<0.05) in plasma levels of TC and HDL-C by 15.41% and 35.10%, respectively, as well as a significant increase (P<0.05) in plasma TG by 23.51%. Administration of DSS-treated mice with L. plantarum (10⁸ CFU/mL) resulted in a significant increase (P<0.05) in TC and HDL-C by 9.85% and 34.45%, respectively, as well as a significant decrease (P<0.05) in plasma TG by 7.20%. When compared to the DSS-treated mice, administration of DSS-treated mice with celebrex (10mg/kg) significantly increased TC and HDL-C by 7.14% and 24.66%, respectively, as well as a significant decrease (P<0.05) in plasma TG by 8.57%.

Effect of *L. plantarum* HBUAS68394 and Celebrex on plasma LRG, IL-1β, and IL-12 in treated mice

Table 6 showed the effect of L. plantarum and celebrex on plasma LRG, IL-1β, and IL-12 in normal and DSS-treated mice. When compared to the normal control group, oral administration of DSS (5%) resulted in a significant increase (p<0.05) in plasma LRG, IL-1β, and IL-12 levels by 119.84%, 220.46%, and 81.83%, respectively. However, when compared to the DSS-treated mice, treatment with L. plantarum (10⁸ CFU/mL) resulted in significantly reduced plasma LRG, IL-1β, and IL-12 levels by 31.03%, 73.22%, and 34.97%, respectively. On the other hand, administration of celebrex (10mg/kg) significantly decreased plasma LRG, IL-1β, and IL-12 levels by 22.94%, 134.49%, and 27.04%, respectively, when compared to the DSS-treated control group of mice (P<0.05).

Table 4. Changes in body weight of control and experimental groups of treated mice

No.	Crouns	Body weight of mice (g)/Number of days		
110.	Groups	0	7	15
	C + 1		36.7	42.18
(I)	Control group	$\pm~2.17^{\mathrm{Aa}}$	$\pm 2.59^{Ab}$	$\pm 2.11^{Bc}$
(III)	L. plantarum HBUAS68394 (10 ⁸ CFU/	32.39	37.17	40.65
(III)	mL)	$\pm~2.15^{Aa}$	± 2.66 Ab	$\pm 1.70^{\mathrm{ABc}}$
(III)	DSS (5% in distilled water)	31.68	30.16	27.83
(III)		$\pm~1.58^{Ab}$	±2.33 Ab	±2.08 ^{Ca}
	DSS + L. plantarum HBUAS68394 (10 ⁸	33.58	34.71	39.52
(IV)	CFU/mL)	$\pm 2.96^{Aa}$	±3.16 ^{Aa}	±2.53 ^{Bc}
(1)	DSS Calabray (10 mg/kg)	32.48	35.25	38.69
(V)	DSS + Celebrex (10 mg/kg)	±2.62 ^{Aa}	±2.83 ^{Ab}	±2.19 ^{Ac}

The body weight of mice consuming regular and DSS plus L. plantarum HBUAS68394 and Celebrex during the 15 days. Values are given as mean \pm SD significantly different at $P \le 0.05$ for groups. Small letters are used for comparison between the means within the column. Capital letters are used to compare means within the row. The high significant levels of the parameters were in the order of a < b < c . Data with superscript alphabet "a" are significantly lower than data with superscript alphabet "b" while data with superscript "b" are lower than data with superscript alphabet c at *P< 0.05.

Table 5. Effect of *L. plantarum HBUAS68394*, and celebrex on plasma total cholesterol (TC), triglycrides (TG), and high density lipoptrotein.cholesterol (HDL-C) in treated mice

No.	Groups	TC	TG	HDL
NO.		(mg/dL)	(mg/dL)	(mg/dL)
(I)	Control group	183.6	75.92	37.92
(I)		$\pm~16.55^{d}$	± 5.93 a	± 2.89 °
(II)	L. plantarum HBUAS68394	185.4	76.64	38.14
(II)	(10 ⁸ CFU/mL)	$\pm~10.47^{d}$	± 6.51 a	± 2.89 °
(III)	DSS (5% in distilled water)	155.3	93.77	24.61
(111)		± 7.20 a	$\pm~7.40^{\rm ~d}$	± 2.26 a
	DSS + L. plantarum HBUAS68394	170.6	81.39 ^b	33.09
(IV)	(10 ⁸ CFU/mL)	± 9.69°	± 3.85 ^b	± 2.79 ^b
(1/)	DSS + Colobray (10 mg/kg)	166.4	85.73	30.68
(V)	DSS + Celebrex (10 mg/kg)	± 8.14 ^b	± 4.68 °	$\pm2.06^{b}$

Values represent the mean \pm SE (n=6). Data shown are mean \pm standard deviation of the number of observations within each treatment. Data followed by the same letter are not significantly different at $P \le 0.05$.

Table 6. Effect of *L. plantarum HBUAS68394*, and celebrex on plasma (leucine-rich alpha-2-glycoprotein (LRG), interleukin-1β (IL-1β), and interleukin-12 (IL-12) in treated mice

No.	Groups	LRG	IL-1β	IL-12 (pg/
110.		(ug/mL)	(pg/mL)	mL)
(I)	Control cross	30.53	43.25	273.1
(I)	Control group	$\pm~3.0^{\rm ~a}$	± 4.09 a	± 12.80a
(II)	L. plantarum HBUAS68394 (10 ⁸ CFU/	29.15	41.54	268.2
(II)	mL)	$\pm~2.18^{\mathrm{a}}$	± 4.08 a	± 14.46a
(III)	DSS	67.12	138.6	496.6
(III)	(5% in distilled water)	$\pm 5.33^d$	$\pm~10.17^{\rm d}$	$\pm20.18^d$
	DSS + L. plantarum HBUAS68394 (10 ⁸	46.29	74.92	322.9
(IV)	CFU/mL)	$\pm~2.82^{\rm b}$	± 9.79 ^b	± 13.96 b
(V)	DSS + C-1-1 (10/l)	51.72	97.41	362.3
(V)	DSS + Celebrex (10 mg/kg)	$\pm~3.26^{c}$	± 8.73°	± 16.54°

Values represent the mean \pm SE (n=6). Data shown are mean \pm standard deviation of the number of observations within each treatment. Data followed by the same letter are not significantly different at P \leq 0.05.

The high significant levels of the parameters were in the order of a < b < c < d. Data with superscript alphabet "a" are significantly lower than data with superscript alphabet "b" while data with superscript "b" are lower than data with superscript alphabet "c and d" at *P< 0.05.

Effect of *L. plantarum* HBUAS68394 and Celebrex on colon GSH, SOD, and MDA in treated mice

Table 7 showed the effect of L. plantarum and celebrex on colon GSH, SOD, and MDA in normal and DSS-treated mice. When compared to the normal control group, oral administration of DSS (5%) resulted in a significant increase (P<0.05) in colon levels of MDA by 312.74%, as well as a significant depletion (P<0.05) of colon GSH and SOD by 52.63% and 61.75%, respectively. However, when compared to the DSS-treated mice, treatment with L. plantarum (10⁸ CFU/ mL) resulted in a significantly reduced colon MDA level by 43.57%, as well as a significant increase in colon GSH and SOD by 74.51% and 82.15%, respectively. Furthermore, administration of celebrex (10mg/kg) significantly decreased colon MDA level by 15.71%, as well as a significant increase in colon GSH and SOD by 37.25% and 30.69%, respectively, when compared to the DSS-treated control group of mice (P<0.05).

Effect of *L. plantarum* and Celebrex on plasma cAMP and TNF-α, and colon MPO in treated mice

Table 8 showed the effect of L. plantarum and celebrex on plasma cAMP and TNF-α, and colon MPO in normal and DSS-treated mice. Administration of DSS (5%) significantly increased plasma cAMP and TNF-α, as well as colon MPO by 127.70%, 25.37%, and 435.85%, respectively, compared to the normal untreated

mice (P<0.05). The administration of L. plantarum significantly decreased plasma cAMP and TNF- α , as well as colon MPO by 43.62%, 15.78%, and 45.34%, respectively, compared to the DSS-treated mice (P<0.05). However, the administration of celebrex significantly increased plasma cAMP and TNF- α , as well as colon MPO by 31.89%, 8.98%, and 28.33%, respectively, compared to the DSS-treated mice (P<0.05).

Effect of *L. plantarum* HBUAS68394 and Celebrex on colon NF-κB, TFF3, and HMGB1 gene expression in treated mice

The effect of *L. plantarum* and celebrex on colon NF-κB, HMGB1, and TFF3 in normal and DSStreated mice Figure 5. When compared to the normal control group, oral administration of DSS (5%) resulted in a significant increase (P<0.05) in colon levels of NF-κB and HMGB1 by 658.42% and 424.75%, respectively, as well as a significant depletion (P<0.05) of colon TFF3 by 36.60%. However, when compared to the DSStreated mice, treatment with L. plantarum resulted in a significant reduction in colon NF-κB and HMGB1 by 48.56% and 49.15%, respectively, as well as a significant increase in colon TFF3 by 21.87%. Furthermore, administration of celebrex significantly decreased colon NF-κB and HMGB1 by 50.13% and 64.72%, respectively, as well as a significant increase in colon TFF3 by 9.37%, when compared to the DSS-treated mice (P < 0.05).

Table 7. Effect of <i>L. plantarum HBUAS</i>	\$68394, and Celebrex on colon	GSH, SOD, and MDA in treated mice
---	--------------------------------	-----------------------------------

No.	Groups	GSH (umole/mg tissue)	SOD (50% NBT reduction/min./mg tissue)	MDA (umole/g tissue)
(I)	Control group	16.72 ± 1.50 ^d	$7.06 \\ \pm 0.39^{\rm d}$	10.07 ± 1.02 a
(II)	L. plantarum HBUAS68394 (10 ⁸ CFU/mL)	17.64 ± 1.75 ^d	$7.60 \\ \pm 0.26^{\rm d}$	10.04 ± 0.76 a
(III)	DSS (5% in distilled water)	7.92 ± 0.65 a	2.70 ± 0.28 a	41.56 ± 2.96 ^d
(IV)	DSS + <i>L. plantarum</i> HBUAS68394 (10 ⁸ CFU/mL)	13.84 ± 0.53 °	4.92 ± 0.22°	23.45 ± 1.53 ^b
(V)	DSS + Celebrex (10 mg/kg)	10.91 ± 0.53 b	3.52 ± 0.34 ^b	35.03 ± 2.07°

Values represent the mean \pm SE (n=6). Data shown are mean \pm standard deviation of the number of observations within each treatment. Data followed by the same letter are not significantly different at $P \le 0.05$.

The high significant levels of the parameters were in the order of a < b < c < d. Data with superscript alphabet "a" are significantly lower than data with superscript alphabet "b" while data with superscript alphabet "c and d" at *P< 0.05.

53.88

 $\pm 5.70^{\circ}$

No.	Groups	cAMP (pg/mL)	TNF-α (pg/mL)	MPO (mU/mg tissue)
(I)	Control group	2.96 ± 0.24 ^a	92.36 ± 8.62 ^a	14.03 ± 1.62 ^a
(II)	L. plantarum HBUAS68394 (10 ⁸ CFU/mL)	3.02 ± 0.24 a	91.32 ± 7.63 ^a	13.29 ± 0.94 ^a
(III)	DSS (5% in distilled water)	$6.74 \\ \pm 0.58^{d}$	115.8 ± 6.34 ^d	75.18 ± 4.36 ^d
(IV)	DSS + <i>L. plantarum</i> HBUAS68394 (10 ⁸ CFU/mL)	3.80 ± 0.31 ^b	97.52 ± 8.29 ^b	41.09 ± 3.29 b

Table 8. Effect of *L. plantarum* HBUAS68394, and Celebrex on plasma cyclic adenosine monophosphate(cAMP) and tumor necrosis factor- α (TNF- α), and colon myeloperoxidase (MPO) in treated mice

Values represent the mean \pm SE (n=6). Data shown are mean \pm standard deviation of the number of observations within each treatment. Data followed by the same letter are not significantly different at $P \le 0.05$.

DSS + Celebrex

(10 mg/kg)

4.59

 $\pm~0.28^{c}$

105.4

 $\pm 6.52^{\circ}$

The high significant levels of the parameters were in the order of a < b < c < d. Data with superscript alphabet "a" are significantly lower than data with superscript alphabet "b" while data with superscript "b" are lower than data with superscript alphabet "c and d" at *P< 0.05.

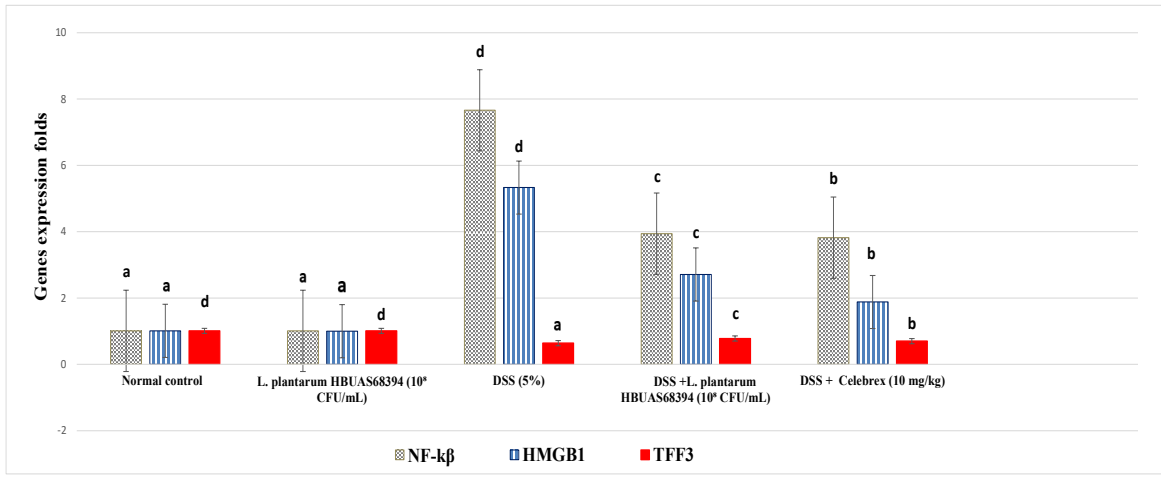


Figure 5. Effect of *L. plantarum* HBUAS68394, and Celebrex on colon Nuclear factor kappa-light-chain-enhancer of activated B cells (NF- κ B), trefoil factor 3 (TFF3), and high mobility group box 1 (HMGB1) gene expression in treated mice. Values represent the mean \pm SE (n=3). Data shown are mean \pm standard deviation of the number of observations within each treatment. Data followed by the same letter are not significantly different at P \leq 0.05.

The high significant levels of the parameters were in the order of a < b < c < d. Data with superscript alphabet "a" are significantly lower than data with superscript alphabet "b" while data with superscript "b" are lower than data with superscript alphabet "c and d" at *P< 0.05.

Effect of *L. plantarum* HBUAS68394 and Celebrex on colon histopathological examination in treated mice

Histopathological changes in colon tissues of normal and *L. plantarum* & celebrex-treated mice were investigated. Histopathological examination in Table 9 and Figure 6 (a & b) showed that groups I and II demonstrated normal morphological structures of the intestinal wall with the colon's lining consisting of mucosa, submucosa, and serosa. The colon mucosa displayed an unchanged

surface coated with columnar epithelium. The crypts appeared to have a linear tubular form. The epithelium is columnar in shape and has clearly visible bordered crypts.

Group III (DSS 5% positive control) exhibited severe damage and disruption in the crypts, which were bordered by small cells containing pyknotic nuclei. An evident increase in goblet cells and lymphatic infiltrations was seen (Table 9 and Figure 6c).

(V)

No.	Groups	Inflammatory cell infiltrate	Erosion (Loss of surfase epithelium)
(I)	Control group	-	-
(II)	L. plantarum HBUAS68394 (108 CFU/mL)	-	-
(III)	DSS (5% in distilled water)	++	+++
(IV)	DSS + L. plantarum HBUAS68394 (108 CFU/mL)	+	+
(V)	DSS + Celebrex (10mg/kg)	+	+

Table 9. Effect of L. plantarum HBUAS68394, and Celebrex on colon histopathological changes in HFD-treated mice

Scoring: (-) indicates normal, (+) indicates mild, (++) indicates moderate, (+++) indicates high.

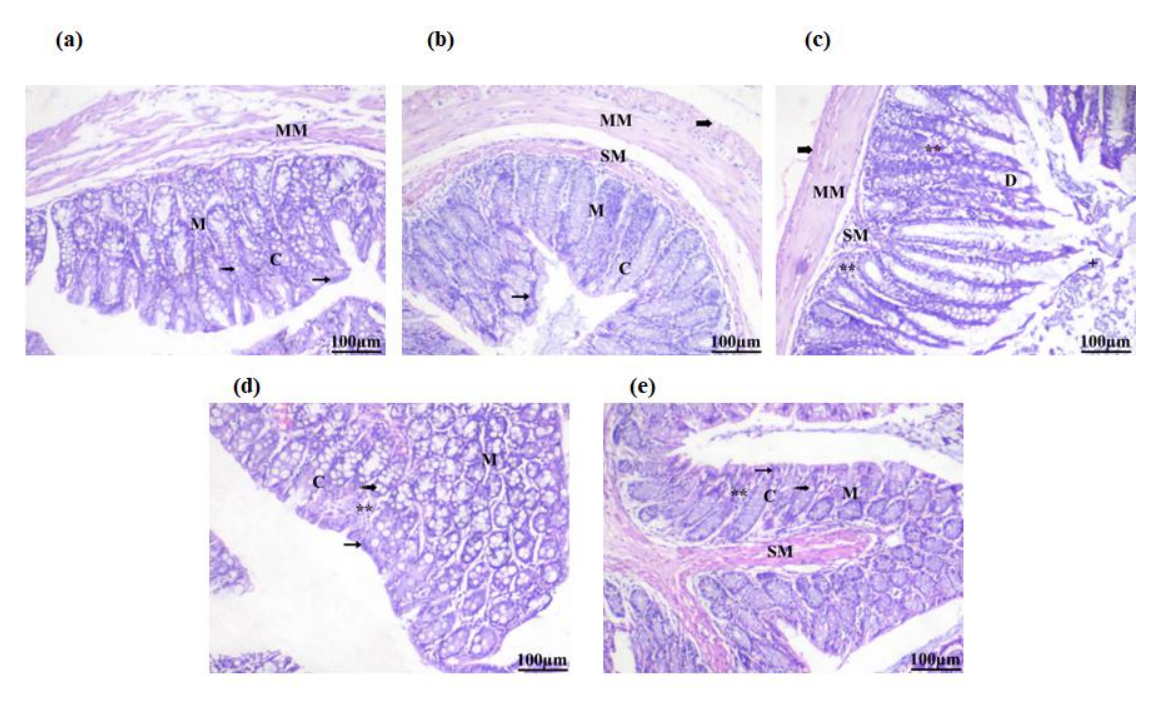


Figure 6. Microscopic pictures of H&E-stained colon sections. (a): Group I, normal group feed regular diet; (b): Group II: Was administrate L. plantarum HBUAS68394 (10⁸ CFU/mL); (c): Group III: Was administrate DSS (5%); (d): Group IV: Was administrate DSS + L. plantarum HBUAS68394 (10⁸ CFU/mL); (e): Was administrate DSS + Celebrex (10 mg/kg). [Intact mucosa (M), submucosa (SM), musculosa (MM), and serosa (bold arrow), crypts (C) with goblet cells (dotted arrow) and surface-simple columnar absorptive epithelial cells (arrow), mucosa (M), mononuclear cells (**), injured crypts (D), surface epithelial cells (notch arrow), and pyknotic nuclei (wavy arrow)]

Table 8 and Figure 6d showed a substantial degree of enhancement in Group IV (DSS + *L. plantarum*), exhibiting an intact mucosa, submucosa, and serosa characterized by nearly typical, well-structured, and closely linked crypts with goblet cells and surface-simple columnar absorptive epithelial cells.

Group V (DSS + celebrex) showed that the mucosa appeared to be intact, with crypts lined with a single layer of columnar epithelium and goblet cells. The architecture of the muscularis mucosa and submucosa was mostly comparable to that of the control group. The observed folds and

crypts appeared to be in normal condition, with a reduced number of cells causing inflammation (Table 9 and Figure 6e).

DISCUSSION

Phylogenetic analysis of the 16S rRNA gene sequence demonstrated that our *L. plantarum* isolate shares 99.35% sequence identity with *L. plantarum*. The 1500 bp genetic marker proved highly effective for strain identification, confirming the utility of this ribosomal RNA region for bacterial classification. The conserved nature of 16S rRNA sequences permits reliable phylogenetic comparisons, while variable

regions enable species-level discrimination (Janda & Abbott, 2007). Our bioinformatics approach utilized BLAST alignment against the comprehensive GenBank database, followed by phylogenetic tree construction to establish taxonomic relationships (Fidanza et al., 2021).

The strain displayed exceptional gastrointestinal adaptability, particularly regarding bile salt resistance. Multiple biochemical adaptations contribute to this tolerance, including bile salt hydrolase enzymes that modify bile acid structure, protective proteins that mitigate oxidative damage and specialized transport mechanisms for stress response (Hamon et al., 2011).

Cell surface characterization revealed distinct adhesion patterns to various solvents. Notably, the strain showed preferential binding to hydrophobic compounds (ethyl acetate and n-hexadecane), with increasing affinity over time. This time-dependent enhancement suggests dynamic modifications to surface properties during environmental exposure. Safety assessment confirmed the non-pathogenic nature of the strain through absence of haemolytic activity on blood agar plates, a key requirement for probiotic applications.

The experimental results demonstrated distinct effects on body weight regulation across treatment groups. While *L. plantarum* administration did not significantly alter body weight in healthy mice, it produced notable effects in the DSS-induced colitis model. DSS treatment caused substantial weight reduction, which was effectively counteracted by both *L. plantarum* supplementation and Celebrex treatment. These findings indicate that probiotic intervention can ameliorate colitis-associated weight loss through multiple pathways.

The metabolic improvements appear mediated through several interconnected mechanisms; Anti-inflammatory Action: Significant reduction in pro-inflammatory cytokines, gut barrier Reinforcement; enhanced intestinal integrity preventing endotoxin translocation, microbial Modulation: Restoration of beneficial gut microbiota populations (Rahayu et al., 2021).

DSS administration induced marked dyslipidaemia, characterized by reduced total cholesterol and HDL-C , elevated triglyceride levels.

These metabolic disturbances result from a cascade of pathological events: epithelial barrier Disruption: Increased intestinal permeability permits bacterial translocation, systemic

Inflammation: Triggered by pathogen-associated molecular patterns, absorptive impairment: Damaged gut mucosa reduces nutrient uptake, microbial dysbiosis: Altered gut microbiota composition affects lipid metabolism (Talley et al., 2021).

L. plantarum administration improved lipid profiles through bile acid metabolism: conjugation reduces cholesterol excretion, triglyceride regulation; modulation of lipid processing pathways, anti-inflammatory effects; systemic inflammation reduction, and microbiome Restoration; promotion of beneficial lipid-metabolizing bacteria.

These findings collectively demonstrate that *L. plantarum* supplementation can effectively counteract the metabolic disturbances associated with experimental colitis through multifaceted mechanisms involving inflammation control, gut barrier protection, and microbial ecosystem restoration.

The experimental model revealed that DSS administration induces colonic inflammation through multiple mechanisms. DSS primarily disrupts epithelial tight junctions, increasing intestinal permeability and facilitating bacterial translocation (Banna et al., 2017). This breach of mucosal integrity triggers systemic inflammation characterized by elevated pro-inflammatory cytokines that subsequently alter lipid metabolism (Leser & Baker, 2024).

L. plantarum demonstrated comprehensive protective effects through three principal mechanisms; immunomodulation: Significant reduction in inflammatory cytokines via T-cell response modulation (Kageyama et al., 2022), oxidative stress mitigation: Enhancement of endogenous antioxidant systems (Tian et al., 2019), and microbiome regulation: Restoration of microbial balance and production of beneficial metabolites (Tang et al., 2016)

While both interventions showed efficacy, their mechanisms differed substantially. *L. plantarum* provided broader ecological benefits including microbiome stabilization, whereas the pharmaceutical agent offered more immediate anti-inflammatory effects through COX-2 inhibition.

At the molecular level, *L. plantarum* administration; downregulated pro-inflammatory signaling pathways, enhanced mucosal repair mechanisms, and restored redox balance

The findings suggest that probiotic interventions may complement conventional therapies by addressing multiple aspects of disease pathogenesis. The ability to modulate both inflammatory responses and microbial ecology positions *L. plantarum* as a promising therapeutic agent for inflammatory bowel conditions.

This integrated analysis of physiological, molecular, and microbial parameters provides a robust foundation for future clinical translation. Subsequent research should investigate optimal dosing strategies and potential synergies with existing treatments to maximize therapeutic benefits.

The experimental data revealed that DSS administration markedly upregulated inflammatory mediators (NF-kB and HMGB1) while suppressing the mucosal protective factor TFF3, indicating both inflammatory activation and impaired barrier function. *L. plantarum* treatment effectively reversed these pathological changes, demonstrating dual anti-inflammatory and tissue-repairing properties through coordinated modulation of these molecular pathways.

L. plantarum downregulated NF- κ B and HMGB1, key regulators of pro-inflammatory cytokines (TNF- α , IL-1 β), likely via modulation of gut microbiota and direct inhibition of nuclear translocation.

The drug's weaker effect on oxidative stress (GSH, SOD) versus *L. plantarum* may stem from its primary action on prostaglandin synthesis rather than antioxidant enzyme induction (Lu et al., 2020).

Histological examination of DSS-treated animals showed characteristic colonic damage including; architecture crypt disruption, goblet cell hyperplasia, pronounced lymphocytic infiltration These morphological alterations were associated with elevated oxidative stress markers, reflecting an imbalance between ROS production and antioxidant defenses.

Therapeutic interventions produced distinct protective effects; *L. plantarum* restored mucosal architecture by reestablishing crypt organization, reducing inflammatory infiltrates, enhancing tight junction protein expression (Mosaad et al., 2016), and celecoxib preserved tissue integrity through alternative mechanisms.

Correlative molecular analyses strengthened these

histological observations; inflammatory marker quantification confirmed treatment efficacy, oxidative stress parameters (MDA, GSH, SOD) reflected redox balance restoration (El Gizawy et al., 2021), and gene expression profiles validated mechanistic pathways (Shehata et al., 2015; Soliman et al., 2022).

The integrated experimental approach, combining; histopathological assessment, Molecular biomarker analysis, and gene expression profiling provided comprehensive validation of treatment effects, with particular emphasis on *L. plantarum's* ability to simultaneously address multiple aspects of colitis pathogenesis (Abdel-Gawad et al., 2003; Hussein, 2013).

CONCLUSION

This study demonstrates that L. plantarum HBUAS68394 effectively mitigates induced colitis by restoring gut barrier integrity, modulating inflammatory responses, and reducing oxidative stress. The probiotic significantly improved colonic histopathology, downregulated pro-inflammatory cytokines (NF-κB, HMGB1), and enhanced mucosal protection (TFF3), while maintaining a favorable safety profile. Comparative analysis revealed that L. plantarum not only matched the anti-inflammatory efficacy of celecoxib but also provided additional benefits in microbiome modulation and tissue repair. These findings highlight the strain's multi-targeted therapeutic potential for inflammatory bowel diseases, supported by integrated molecular, biochemical, and histological evidence, warranting further clinical exploration of its translational applications.

Significance of the study

- Comprehensive analysis: The study integrates histological analysis with molecular data and various biochemical parameters to provide a thorough understanding of the treatments' efficacy.
- **Gut Barrier function**: *L. plantarum* was found to enhance gut barrier function, modulate gut microbiota, and reduce pro-inflammatory cytokines.
- Inflammation reduction: Celebrex effectively maintained tissue integrity and reduced inflammation.
- Future applications: The insights gained pave the way for future clinical applications and personalized treatment strategies

for inflammatory bowel diseases (IBD).

Competing interests: The authors declare no conflict of interest, financial or otherwise.

Authors' contributions: Fatma E.A. Yousef: Oversaw study design, coordination, and contributed to histological analysis and result interpretation: Mohammed A. Hussein: Conceptualized the study, secured funding, supervised experimental procedures, and was involved in PCR and biochemical assays; Reda M. Taha: Contributed to experimental design and execution, focusing on oxidative stress biomarkers and lipid metabolism, and assisted in data analysis; Mai A. Mwaheb: Handled day-today laboratory work, including mouse treatment, sample collection, various assays, and contributed to histological analysis and data collection.

Ethical committee: The study was approved by the Fayoum University Institution Animal Care and Use Committee (FU-IACUC) under approval No. EAC2370-a, ensuring all procedures were conducted according to ethical standards.

Funding: The authors are not currently in receipt of any research funding.

REFERENCES

- Abbasiliasi, S., Tan, J.S., Bashokouh, F., Ibrahim, T.A.T., Mustafa, S., Vakhshiteh, F. et al. (2017). In vitro assessment of *Pediococcus acidilactici* Kp10 for its potential use in the food industry. *BMC Microbiology*, 121: 1–11.
- Abdel-Gawad, S.M., Ghorab, M.M., El-Sharief, A.M.S., El-Telbany, F.A., Abdel-Alla, M. (2003). Design, synthesis, and antimicrobial activity of some new pyrazolo[3,4-d] pyrimidines. *Heteroatom Chemistry*, 14: 530-534.
- Banna, G.L., Torino, F., Marletta, F., Santagati, M., Salemi, R., Cannarozzo, E., et al. (2017). Lactobacillus rhamnosus GG: An overview to explore the rationale of its use in cancer. Frontiers in Pharmacology, 8: 603. doi: 10.3389/ fphar.2017.00603.
- Creighton, C.J., Fountain, M.D., Yu, Z., Nagaraja, A.K., Zhu, H., Khan, M., et al. (2010). Molecular profiling uncovers a p53-associated role for microRNA-31 in inhibiting the proliferation of serous ovarian carcinomas and other cancers. *Cancer Research*, 70(5): 1906-15.
- Danese, S. (2011). New therapies for inflammatory bowel disease: from the bench to the bedside. *GUT*, 61(6): 918-32.

- El Gizawy, H.A., Abo-Salem, H.M., Ali, A.A., Hussein, M.A. (2021). Phenolic profiling and therapeutic potential of certain isolated compounds from *Parkia roxburghii* against AChE activity as well as GABAA α5, GSK-3β, and p38α MAP-kinase gene. *ACS Omega*, 6(31): 20492–20511.
- Fidanza, M., Panigrahi, P., Kollmann, T.R. (2021). Lactiplantibacillus plantarum-nomad and ideal probiotic. Frontiers in Microbiology, 12: 712236. doi: 10.3389/fmicb.2021.712236.
- Ghosh, S., Mitchell, R. (2007). Impact of inflammatory bowel disease on quality of life: Results of the European Federation of Crohn's and Ulcerative Colitis Associations (EFCCA) patient survey. *Journal of Crohn's and Colitis*, 1(1): 10-20.
- Hamon, E., Horvatovich, P., Izquierdo, E. et al. (2011). Comparative proteomic analysis of *Lactobacillus plantarum* for the identification of key proteins in bile tolerance. *BMC Microbiology*, 11: 63. https://doi.org/10.1186/1471-2180-11-63.
- Hussein, M.A. (2013). Prophylactic effect of resveratrol against ethinylestradiol-induced liver cholestasis. *Journal of Medicinal Food*, 16(3): 246-254.
- Ilavenil, S., Kim, D.H., Valan Arasu, M., Srigopalram, S., Sivanesan, R., Choi, K.C. (2015). Phenyllactic acid from *Lactobacillus plantarum* promotes adipogenic activity in 3T3-L1 adipocyte via Upregulation of PPAR-γ2. *Molecules*, 20(8): 15359-73.
- Janda, J.M., Abbott, S.L. (2007). 16S rRNA gene sequencing for bacterial identification in the diagnostic laboratory: Pluses, perils, and pitfalls. *Journal of Clinical Microbiology*, 45(9): 2761-2764.
- Kageyama, Y., Nishizaki, Y., Aida, K., Yayama, K., Ebisui, T., Akiyama, T., et al. (2022). Lactobacillus plantarum induces innate cytokine responses that potentially provide a protective benefit against COVID-19: A single-arm, double-blind, prospective trial combined with an in vitro cytokine response assay. Experimental and Therapeutic Medicine, 23(1): 20. doi: 10.3892/etm.2021.10942.
- Leite, A.M.O., Miguel, M.A.L., Peixoto, R.S., Ruas-Madiedo, P., Paschoalin, V.M.F., et al. (2015). Probiotic potential of selected lactic acid bacteria strains isolated from Brazilian kefir grains. *Journal of Dairy Science*, 98(6): 3622–3632.
- Leser, T., Baker, A. (2024). Molecular mechanisms of *Lacticaseibacillus rhamnosus*, LGG® probiotic function. *Microorganisms*, 12(4): 794. https://doi.org/10.3390/microorganisms12040794.

- Li, Y., Ma, M., Wang, X., Li, J., Fang, Z., Li, J., et al. (2024). Celecoxib alleviates the DSS-induced ulcerative colitis in mice by enhancing intestinal barrier function, inhibiting ferroptosis and suppressing apoptosis. *Immunopharmacology and Immunotoxicology*, 46(2): 240-254.
- Lu, P.D., Zhao, Y.H. (2020). Targeting NF-κB pathway for treating ulcerative colitis: Comprehensive regulatory characteristics of Chinese medicines. *Chinese Medicine*, 15: 15. https://doi.org/10.1186/s13020-020-0296-z
- Mendoza, S.N., Olivier, B.G., Molenaar, D., Teusink, B. (2019). A systematic assessment of current genome-scale metabolic reconstruction tools. *Genome Biology*, 20(1): 158. doi: 10.1186/s13059-019-1769-1.
- Metwaly, A., Elmoghazy, H., Hussein, M., Abdel-Aziz, A., Elmasry, S. (2022). CAPE Improves Vanin-1/AKT/miRNA-203 Signaling Pathways in DSS-induced Ulcerative Colitis. *Biomedical Research and Therapy*, 9(9): 5313-5325.
- Mosaad, Y.O., Gobba, N.A., Hussein, M.A. (2016). Astaxanthin; a promising protector against gentamicin-induced nephrotoxicity in rats. *Current Pharmaceutical Biotechnology*, 17(13): 1189-1197.
- Muro, P., Zhang, L., Li, S., Zhao, Z., Jin, T., Mao, F., et al. (2024). The emerging role of oxidative stress in inflammatory bowel disease. *Frontiers* in *Endocrinology*, 15: 1390351. doi: 10.3389/ fendo.2024.1390351.
- Nakov, R., Velikova, T., Nakov, V., Ianiro, G., Gerova, V., Tankova, L. (2019). Serum trefoil factor 3 predicts disease activity in patients with ulcerative colitis. European Review for Medical and Pharmacological Sciences, 23(2): 788-794.
- Nordström, E.A., Teixeira, C., Montelius, C., Jeppsson, B., Larsson, N. (2021). *Lactiplantibacillus* plantarum 299v (LP299V®): Three decades of research. *Beneficial Microbes*, 12(5): 441-465.
- Rahayu, E.S., Mariyatun, M., Putri Manurung, N.E., Hasan, P.N., Therdtatha, P., et al. (2021). Effect of probiotic *Lactobacillus plantarum* Dad-13 powder consumption on the gut microbiota and intestinal health of overweight adults. *World Journal of Gastroenterology*, 27(1): 107-128.
- Satohiro, M., Hirosato, M. (2022). Usefulness of the optimal cutoff value and delta value of leucine-rich alpha 2 glycoprotein in ulcerative colitis. *Crohn's & Colitis*, 4: 1-6.
- Shehata, M.R., Mohamed, M.M.A., Shoukry, M.M.,

- Hussein, M.A., Hussein, F.M. (2015). Synthesis, characterization, equilibria and biological activity of dimethyltin (IV) complex with 1,4-piperazine. *Journal of Coordination Chemistry*, 68(6): 1101-1114.
- Soliman, S.M., Mosallam, S., Mamdouh, M.A., Hussein, M.A., Abd El-Halim, S.M. (2022). Design and optimization of cranberry extract loaded bile salt augmented liposomes for targeting of MCP-1/STAT3/VEGF signaling pathway in DMN-intoxicated liver in rats. *Drug Delivery*, 29(1): 427-439.
- Takahiro, S., Takayuki, Y., Shigeyuki, Y., Ryutaro, N., Satoru, U. (2023). Leucine-rich alpha-2 glycoprotein is a reliable serum biomarker for evaluating clinical and endoscopic disease activity in inflammatory bowel disease. *Inflammatory Bowel Diseases*, 29: 1399–1408.
- Talley, S., Valiauga, R., Anderson, L., Cannon, A. R., Choudhry, M.A., et al. (2021). DSS-induced inflammation in the colon drives a proinflammatory signature in the brain that is ameliorated by prophylactic treatment with the S100A9 inhibitor paquinimod. *Journal of Neuroinflammation*, 18(1). https://doi.org/10.1186/s12974-02102317-6
- Tang, W., Xing, Z., Hu, W., Li, C., Wang, J., Wang, Y. (2016). Antioxidative effects in vivo and colonization of Lactobacillus plantarum MA2 in the murine intestinal tract. *Applied Microbiology and Biotechnology*, 100(16): 7193-202.
- Tian, X., Yu, Z., Feng, P., Ye, Z., Li, R., Liu, J., Hu, J., et al. (2019). *Lactobacillus plantarum* TW1-1 alleviates diethylhexylphthalate-induced testicular damage in mice by modulating gut microbiota and decreasing inflammation. *Frontiers in Cellular and Infection Microbiology*, 9: 221. doi: 10.3389/fcimb.2019.00221.
- VanPatten, S., Al-Abed, Y. (2018). High mobility group Box-1 (HMGb1): Current wisdom and advancement as a potential drug target. *Journal of Medicinal Chemistry*, 61(12): 5093-5107.
- Yang, Y., Lin, Z., Lin, Q., Bei, W., Guo, J. (2022). Pathological and therapeutic roles of bioactive peptide trefoil factor 3 in diverse diseases: Recent progress and perspective. *Cell Death and Disease*, 13(1): 62. doi: 10.1038/s41419-022-04504-6.